琉球大学学術リポジトリ

Numerical simulation of the stress field along the project INDEPTH profile: implication for the deep crustal relations between the MCT, STD and GCT

メタデータ	言語: 出版者: 琉球大学理学部 公開日: 2011-11-09 キーワード (Ja): キーワード (En): 作成者: Matrika Prasad, Koirala, Hayashi, Daigoro, 林, 大五郎 メールアドレス: 所属:
URL	http://hdl.handle.net/20.500.12000/22087

Numerical simulation of the stress field along the project INDEPTH profile: implication for the deep crustal relations between the MCT, STD and GCT

*Matrika Prasad Koirala and Daigoro Hayashi

Simulation Tectonics Laboratory
Faculty of Science
University of the Ryukyus, Okinawa, 903-0129, Japan

Abstract

Many interesting findings were obtained during the INDEPTH geophysical surveys but the results of these surveys were not sufficient to explore the deep crustal relations among the Himalayan Mega Thrust namely MCT, STD and GCT. In this study, 2-D finite element method was used to analyze the state of stress and deep crustal relation between MCT, STD and GCT. Elasto-plastic, plane strain model constrained by the northward convergent displacement boundary condition was used to simulate the stress field. Modelling results reveal that thrust/fault geometry, their deep crustal relations and how do they terminate had effect on the stress field, displacement vector, shear stress and exhumation. The lateral variation of the stress orientation and surface exposure of fault/thrust and lithologic units may be the expression of the deep crustal relations between the major structures, their geometry and how do they terminate at the depth. So the along strike variation in the Himalaya may be the manifestation of structural geometry and their deep crustal relationships.

Introduction

The Himalayan orogen is defined by the Indus-Tsangpo suture in north, the left-slip Chaman fault in the west, the right-slip Sagaing fault in the east, and the Main Frontal Thrust in South (Lefort, 1975).

The Himalayan tectonic system is a broader concept than the Himalayan orogen. It consists of the Himalayan orogen, the active Himalayan foreland basin (=Indo-Gangetic Depression), and the Indus and Bengal Fans. All of these features were produced by the Cenozoic Indo-Asian Collision (Yin, 2006).

Despite the long research history (over 150 Yrs), the geometry, kinematics and dynamic evolution of the Himalayan orogen remain poorly understood (Yin, 2006). Although, roughly, the mega thrust system and the stratigraphic units between these structures are comparable throughout the Himalaya, there is along strike variations in stratigraphic juxtapositions, metamorphic grades, crustal shortening, slip magnitudes, geometry of the mega thrust and their probable relations in depth.

Main Central Thrust (MCT) has flat ramp geometry in central Nepal, in the western Himalaya MCT exhibits only a major lateral ramp. Everywhere exposed, the South Tibetan Detachment (STD) follows roughly the same stratigraphic horizon at the base of the Tethyan Himalayan Sequence (THS), exhibiting a long (>100km) hanging wall flat. This relationship suggests that the STD may have initiated along a pre-existing lithologic contact or the subhorizontal brittle-ductile transition zone in the middle crust (Yin 2006).

The southernmost trace of the STD either merges with the MCT (e.g., Zanskar) or lies within 1-2 km of the MCT frontal trace (e.g. in Bhutan), suggesting that the MCT may join the STD in their up-dip directions to the south. This geometry, largely neglected by the existing

Received: August 31, 2011
* E-mail: matrikakoirala@gmail.com

models, has important implications for the deformation, exhumation and the sedimentation history of the entire Himalayan orogen (Yin, 2006).

The origin of North Himalayan gneiss domes and the east-trending North Himalayan antiform (NHA) are uncertain largely due to the fact that the deep crustal relationships among the MCT, STD, and GCT are poorly constrained. Results from INDEPTH surveys are inconclusive; the STD could either join the MCT downward along the Main Himalayan Thrust or flatten into a ductile shear zone in the middle crust. The first interpretation would support the prediction of the wedge extrusion model while the second would permit channel flow of Tibetan lower crust to the Himalaya. It is also possible that the STD links with the coeval Great Counter Thrust via a subhorizontal shear zone in the middle crust beneath the Himalaya (Yin, 2006 and references therein).

Numerical Simulation is a powerful tool to analyze the deep crustal processes. Finite element method (FEM) is one of the robust methods to simulate the state of stress and resulting deformation (Mäkel and Walters, 1993; Zhao et al., 2004; Liu and Li, 2006; Manglik et al., 2008; Koirala and Hayashi, 2008; Koirala and Hayashi, 2009; Luo and Liu, 2009). The state of stress and resulting deformation are important to explore the faulting pattern and tectonics of the area (Cai and Wang, 2001; Lynch and Richards, 2001; Malservisi et al., 2003; Flesch et al., 2007; Koirala and Hayashi, 2008; Koirala and Hayashi, 2010). Direct observations and geophysical observations only are not sufficient to analyze the deep crustal processes. Many numerical methods like finite element, finite difference and potential field etc are popular in Earth Science. In this study, plane strain finite element elasto-plastic models are created to analyze the effect of the deep crustal relations among the MCT, STD and GCT. Three models are created with the geometrical variation of these structures and how do they terminate (Figure 1). These models are based on modified INDEPTH section of Nelson et al., 1996. This study aims to understand the effect of the geometry and structural relationships among the MCT, STD and GCT.

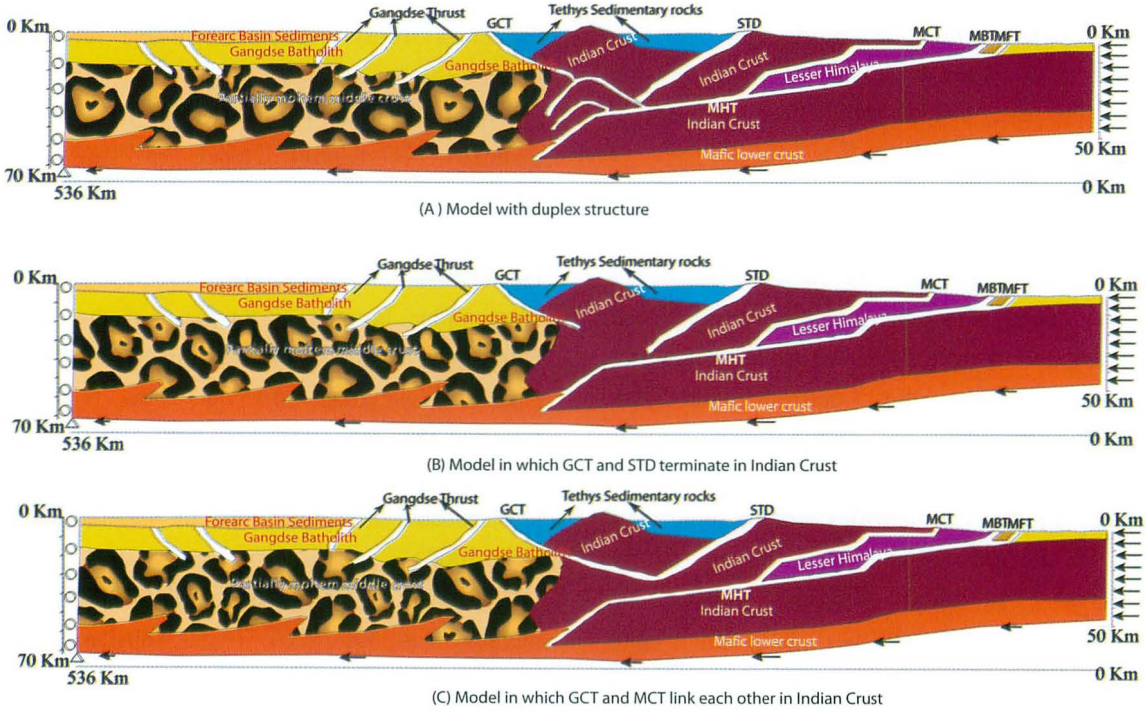

Fig. 1. Geological Cross-Section along the Project INDEPTH, Geometry and Boundary Conditions (A) Model with duplex structure (B) Model in which GCT and STD terminate in Indian Crust (C) Model in which GCT and STD link each other in Indian Crust.

Tectonic Setting and description of the structures

In general all the major structures are found laterally throughout the Himalayas but sometimes stratigraphic position of the structures and names are different in different locations. Main Frontal Thrust (MFT), Main Boundary Thrust (MBT), Main Central Thrust (MCT) and South Tibetan Detachment (STD) are the major structures found from south to north in the Himalaya. Main Himalayan Thrust (MHT) is low angle fault where major Himalayan thrust (MFT, MBT, and MCT) sole in to it. MHT was first purposed by Schelling and Arita (1991) as Main Detachment Fault (MDF) based on structural reconstruction of Eastern Himalaya of South Himalaya and later it was termed as MHT by Zhao et al., 1993 and Nelson et al., 1996 based on their INDEPTH seismic reflection profiles in the North Himalaya. Great Counter Thrust (GCT) is a south dipping structure just south of the Indus-Tsangpo suture zone. It is also known as Renbu-Zedong thrust or Himalayan Backthrust in southern Tibet (Heim and Gansser, 1939; Ratschbacher et al., 1994; Yin et al., 1994, 1999). Readers are referred to Hodges (2000), Upreti (1999) and Yin (2006) for the detailed of the tectonic setting, geology and structures.

Simulation Model

In order to simulate the role of structural geometry and their deep crustal relationships among the MCT, STD and GCT on the deformation in the Himalaya, three models were created based on the modified interpretative section of Nelson et al., 1996 (Fig. 1). Simulations performed in this study were calculated by using the FE software package developed by Hayashi (2009). Progressive compressive displacement boundary condition was used (Fig. 1) to simulate the India-Eurasia Convergence. Young's modulus, density, Poisson's ratio, yield strength and strain hardening were used to constrain the material properties (Fig. 2). Case 10 material properties are best fit material properties among the different sets. A total of 15 (3 models) x 5(total cumulative displacement) calculations were performed. General values for these parameters are selected from the available published literature (Bird and Kong, 1994; Cai and Wang, 2001; Chery et al. 2001; Lynch and Richards, 2001; Malservisi et al., 2003; Zhao et al., 2004; Parsons, 2006; Flesch et al. 2007; Manglik et al., 2008; Luo and Liu, 2009; Owens, and Zandit, 1997). Published velocity model of Pandey et al. (1995), Owens and Zandit (1997) and global velocity structures as described in Cheistensen and Mooney (1995) are used to get the Young's modulus using the relationship described by Pauselli and Federico (2003) provided density and Poisson's ratio are fixed by dominant rock type.

Modeling Results

Modeling results are analyzed by using the stress field, displacement vectors and maximum

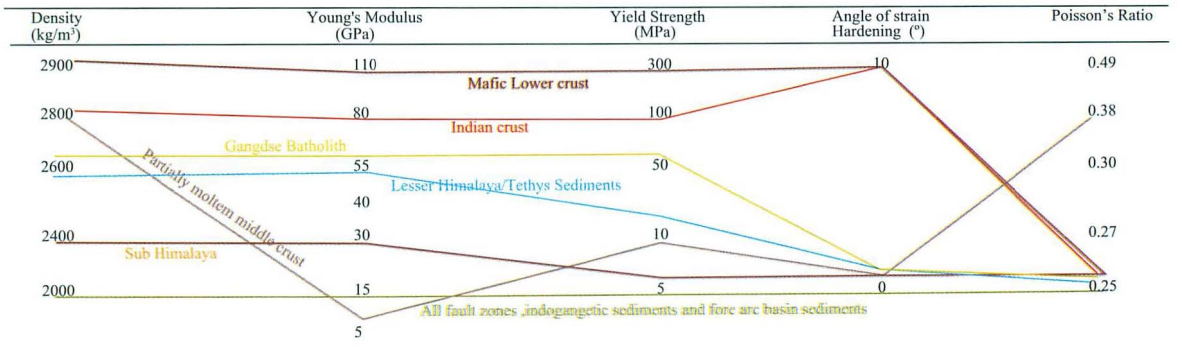

Fig. 2. Rock layer properties applied for models (A), (B) and (C).

shear stress (τ_{max}). In all the cases, maximum principle stress σ_1 is vertical or near to vertical and compressive in the lower part of the model and horizontal in the upper part of the model, which is favorable for the southward propagating thrust fault in the Himalaya. The tensional stress field are obtained in the Himalayan frontal part and along with the frontal thrust zone (mainly the MCT), upper surface of the THS, crest of the North Himalayan Domes, upper surface of the both flank of the North Himalayan Domes and upper surface of the southern Tibet. These tensional stresses are proof of the simultaneous development of extensional tectonics in the upper frontal part of the Himalaya and around the thrust zones as well as development of rift system in the Tibetan Plateau. Some tensional stresses are observed in the sharp angular contact between the mafic lower crust and partially molten middle crust and are the boundary effect as these are not observed in the models with smooth contact.

Stress Field

Stress field for the three models with 1 m displacement (0.1 m increment) and 100 m displacement (1 m increment) are calculated. Figure 3 shows the stress field for the three models with 1 m cumulative displacement. Figure 4 shows the stress field for the three models with 100 m cumulative displacement. For all the figures long lines are the maximum compressive horizontal stress σ_{Hmax} and the short lines are the minimum compressive horizontal stress σ_{Hmin}. The red lines in the figures show the tension and the black lines show the compression. The general trend of the stress field is almost similar in all the models. In general all the models shows compressive state of stress with some tensional stress in the frontal part and thrust fault zones and in the surface of the THS and in the upper surface of the south Tibetan Plateau.

In model (B) the compressive stress around the STD becomes vertical, which is inclined in

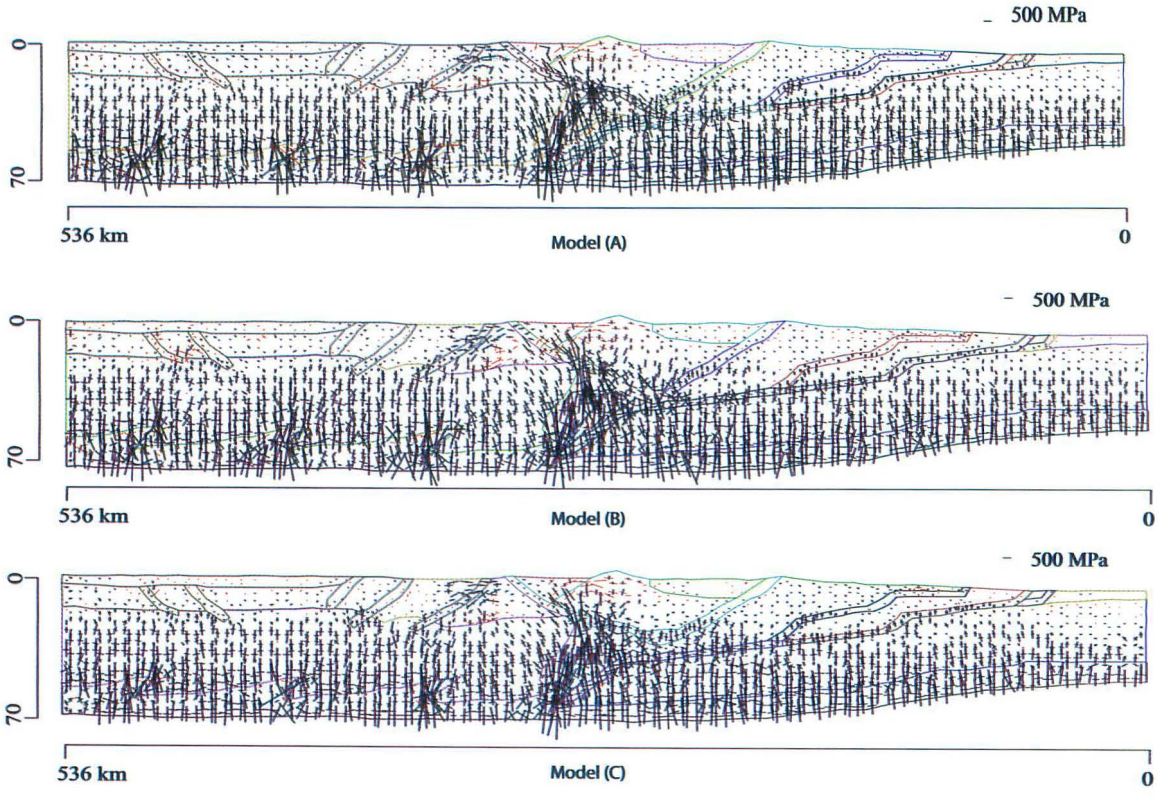

Fig. 3. Stress distribution at 1 m displacement with 0.1 m increment for models (A),(B) and (C) respectively, each pair of perpendicular lines represent $\sigma 1$ (long lines) and $\sigma 3$ (short lines), tensional stresses are represented by red lines.

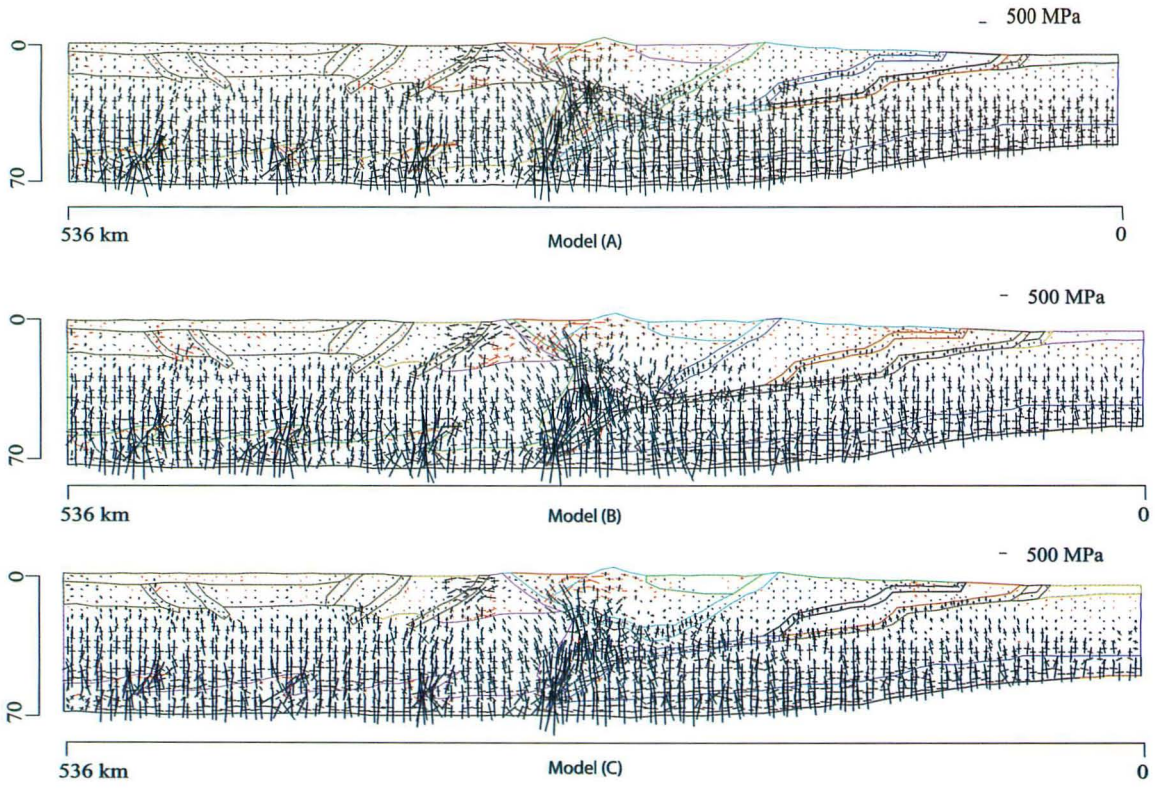

Fig. 4. Stress distribution at 100 m displacement with 1 m increment for models (A),(B) and (C) respectively, each pair of perpendicular lines represent $\sigma 1$ (long lines) and $\sigma 3$ (short lines), tensional stresses are represented by red lines.

model (A). In model (C) the compressive stress at the deeper part of the STD are vertical, but they again becomes inclined in the shallow depth. The tensional stress increases in model (B) than model (A) and (C), around the MCT fault zones. Some tensional stresses are developed just south of the STD in the upper surface of the higher Himalayan rocks. In model (B) and (C), magnitudes of the stress in the upper part of the model decreases than model (A). Tensional stresses in the Higher Himalaya increase in model (C) than models (A) and (B). Tensional stress in upper surface of the MCT fault zones increases in the Model (B) than model (A) and (C). Tensional stresses in the southern Tibet Plateau decrease in the model (B) than model (A) and model (C).

Increasing the displacement from 1 m to 100 m (Figs. 3 and 4) shows that the magnitudes if the stresses in the upper part of the model decreases in all the models. The tensional stress in the upper surface of the model just north of the models decreases. In all the models the tensional stresses are decoupled from the underlying overall compressional stresses. These stress field observed shows that the geometry of the structure at the depth and how do they terminate in the depth effect the overall stress pattern and faulting type, which is well observed in the different section of the Himalayas. So in conclusion, the structures observed in the surface of the model clearly represent the geometry and their relation at the depth.

Maximum Shear Stress (τ_{max})

Maximum shear stress (τ_{max}) for model (A), (B) and (C) at 1 m displacement with 0.1 m increments are shown in the figure 5 and at 100 m displacement with 1 m increment are shown in figure 6. In all the models the maximum shear stress (τ_{max}) are maximum in the deeper part of the models and in front of MHT ramp of the models. Increasing the displacement increases the

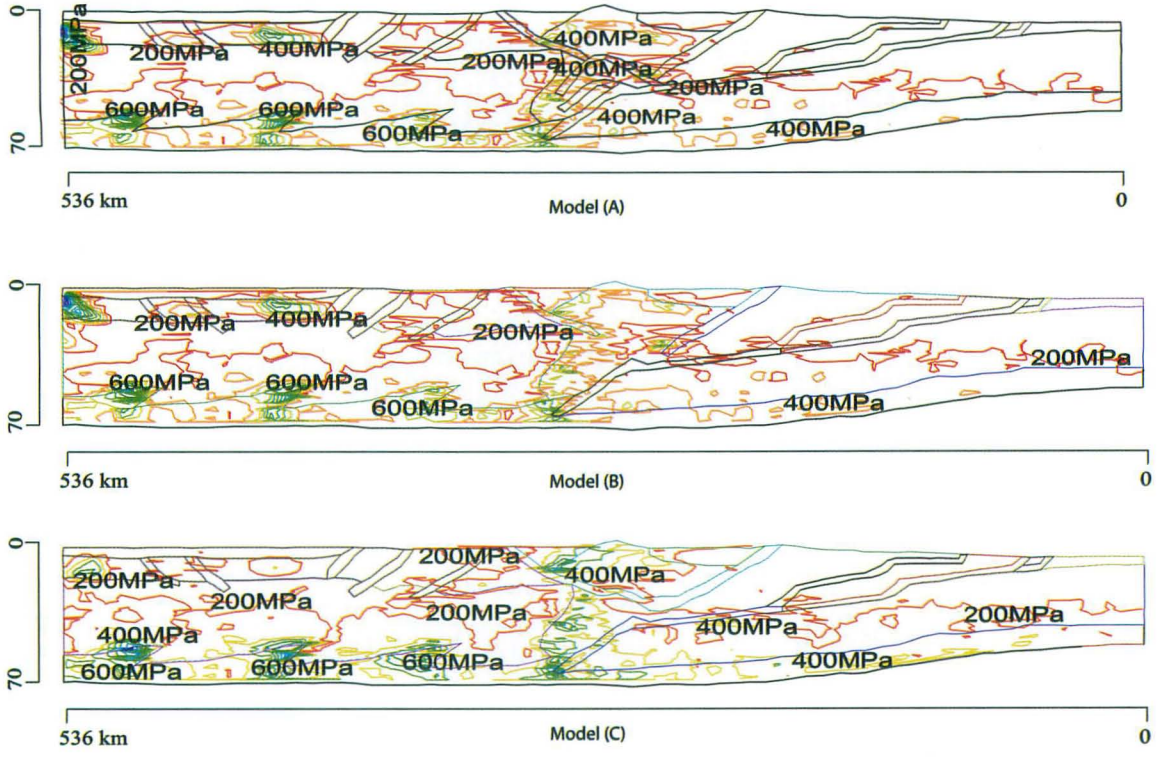

Fig. 5. Shear stress distribution at 1 m displacement with 0.1 m increment for models (A),(B) and (C) respectively.

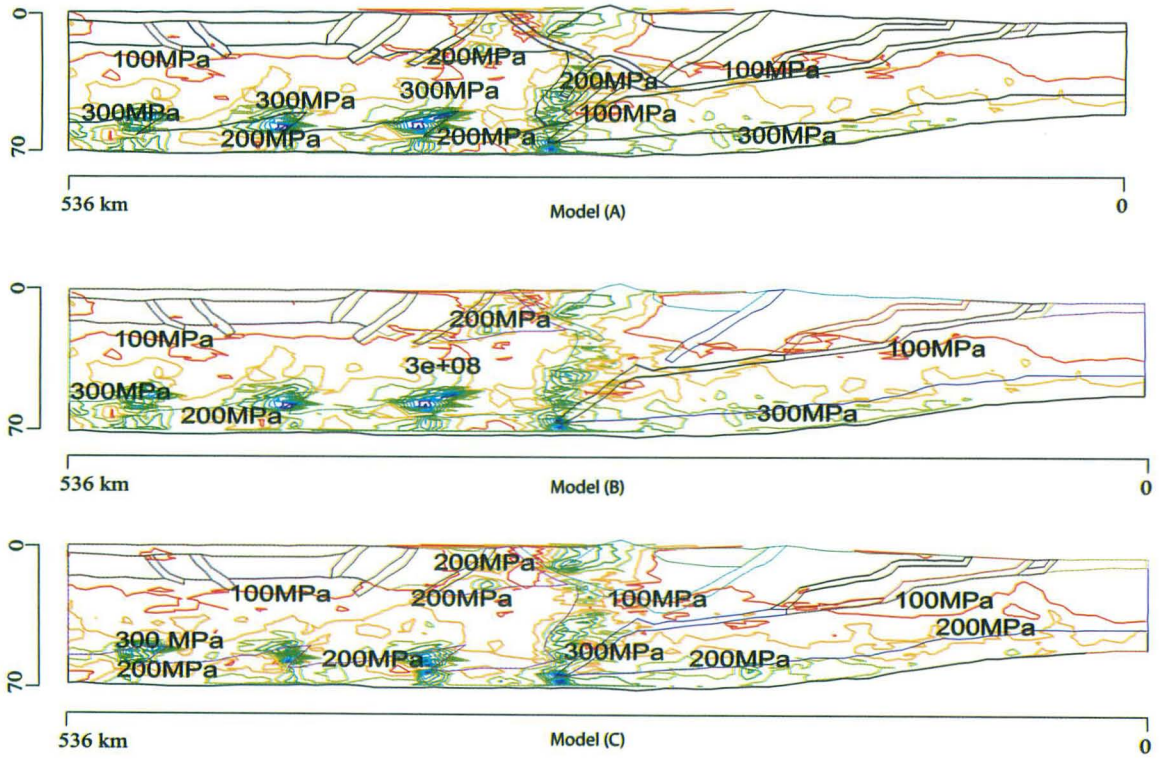

Fig. 6. Shear stress distribution at 100 m displacement with 1 m increment for models (A),(B) and (C) respectively.

magnitudes of the maximum shear stress (τ_{max}) in the deeper part of the model and in front of the MHT ramp.

Maximum shear stress (τ_{max}) increases in front of the MHT ramp and upper part of the GCT in model (C) than in model (A) and (B). In all the models maximum shear stress (τ_{max}) is also concentrated in the sharp bends of the model boundary between the mafic lower crust and partially molten middle crust, which is clearly the boundary effect.

Displacement Vector

Displacement vectors for models (A), (B) and (C) are shown in the figures 7 and 8. Figure 7 shows the displacement vectors for 1 m displacement at 0.1 m increment. Figure 8 shows the displacement vectors at 100 m displacement at 1 m increment. Magnitudes of the displacement vectors are increase in model (B) and (C) than in model (A). Increasing the displacement increase the magnitudes of the displacement vectors in all the models. The displacement vectors north of the GCT are straight and northward in all the models, and are slightly downward and northward towards the partially molten middle crust. The downward trend of the displacement vectors increases in model (B) than in model (A) and further increase in model (C) than model (B). There are slight differences in displacement vectors in front of the MHT ramp in different models.

Discussions

2-D elasto-plastic FE models were created to understand the effect of the geometrical relationships between the major thrust faults in the Himalaya. Three sets of plausible conditions were tested but there may be still other relations that need to be tested. All the layers in the models are homogeneous and isotropic. Best set of material properties are only considered. This modeling only consider the elasto-plastic layering, the viscous layer (mantle) at the depth may

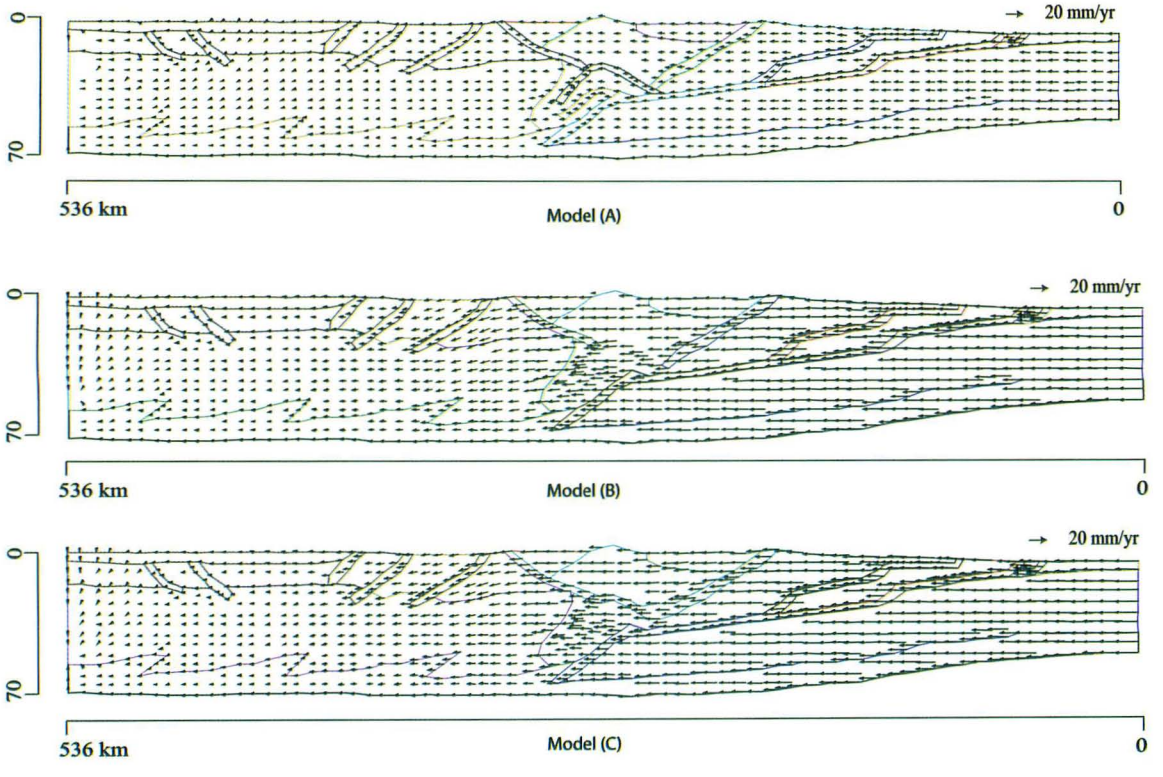

Fig. 7. Displacement vectors at 1 m displacement with 0.1 m increment for models (A),(B) and (C) respectively.

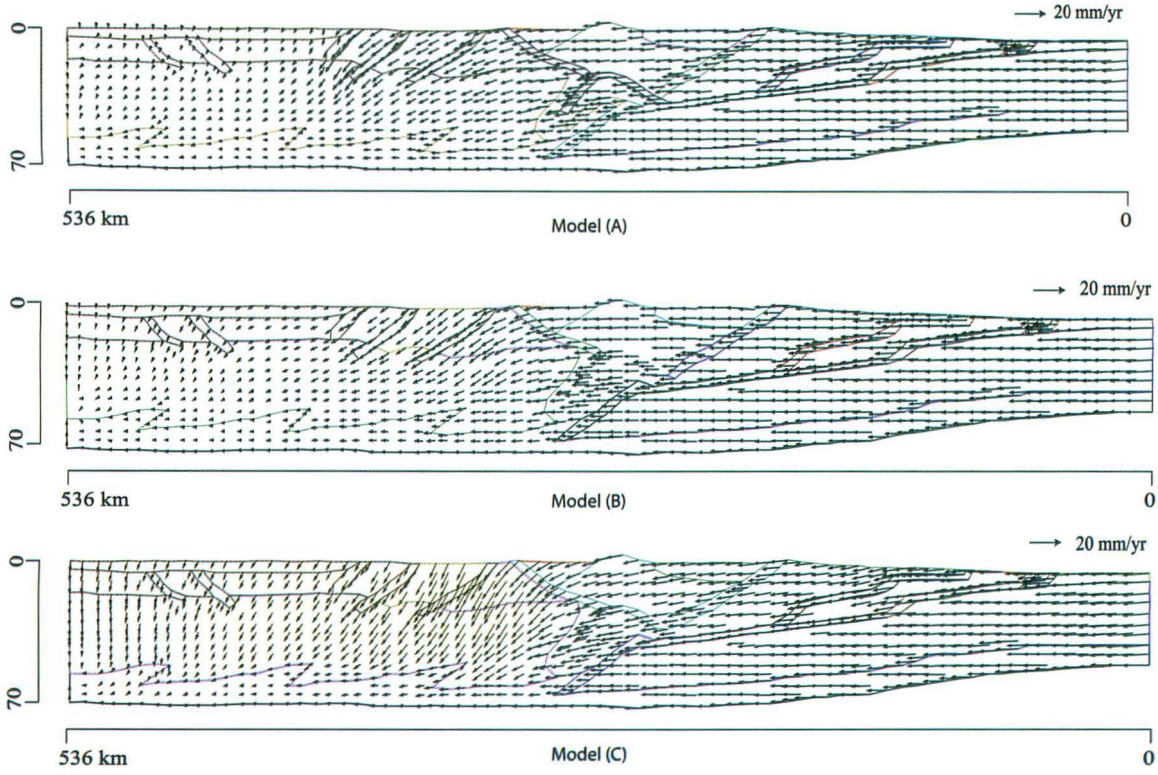

Fig. 8. Displacement vectors at 100 m displacement with 1 m increment for models (A),(B) and (C) respectively.

significantly deviates the results. The models with smooth layer boundary between the mafic lower crust and partially molten middle crust were created to test the effect of sharp bending, as stated earlier there were some effect on the stress field and maximum shear stress (τ_{max}). But these effects were localized only on the sharp bend and they had no effect on other parts of the model.

Conclusions

2-D finite element method was used to analyze the state of stress and deep crustal relation between MCT, STD and GCT. Elasto-plastic, plane strain model constrained by the northward convergent displacement boundary condition was used to simulate the stress field. Young's modulus, density, Poisson's ratio, yield strength and strain hardening were used to constrain the material properties of different layers. General values for these parameters were selected from the available published literature and best fit values from previous studies. Modelling results reveal that thrust/fault geometry, their deep crustal relations and how do they terminate had effect on the stress field, displacement vector, shear stress and exhumation. The lateral variation of the stress orientation and surface exposure of fault/thrust and lithologic units may be the expression of the deep crustal relations between the major structure their geometry and how do they terminate at the depth. So the along strike variation in the Himalaya may be the manifestation of structural geometry and their deep crustal relationships.

Acknowledgements

M. P. K. is grateful to Ministry of Education, Culture, Sports, Science, and Technology, (Monbukagakusho) Japan for the scholarship to carry out this research work under the special graduate program of the Graduate School of Engineering and Science, University of the Ryukyus, Okinawa, Japan.

References

Cai, Y., Wang, C.Y., 2001. Testing fault models with numerical simulation: example from central California. Tectonophysics 343, 233-238.

Cheistensen, N. I., Mooney, W. D., 1995. Seismic velocity and composition of the continental crust: A global view, Journal of geophysical research, 110(B7), 9761-9788.

Flesch, L.M., Holt, W.E., Haines, A.J., Wen, L., Shen-Tu B., 2007. The dynamics of western North America: stress magnitudes and the relative role of gravitational potential energy, plate interaction at the boundary and basal tractions. Geophysical Journal International 169, 866-896. doi: 10.1111/j.1365-246X.2007.03274.x.

Hayashi, D., 2008. Theoretical basis of FE simulation software package. Bulletin of Faculty of Science, University of the Ryukyus, No. 85, 81-95. http://ir.lib.u-ryukyu.ac.jp/.

Hayashi, D., 2009. Theoretical basis of elastoplasticity in FE software package. Bulletin of Faculty of Science, University of the Ryukyus,, No. 88, 9-13. http://ir.lib.u-ryukyu.ac.jp/.

Heim, A., Gansser, A., 1939. Central Himalaya Geological Observations of Swiss, pp. 1-246.

Hodges, K.V., 2000. Tectonics of the Himalaya and southern Tibet from two perspectives. Geological Society America Bulletin 112, 324-350.

Koirala, M. P., Hayashi, D., 2008. Numerical Simulation of the stress field in California, Implication for the present day plate Kinematics. Bollettino di Geofisica teorica ed applicata 49(2 supplement), 60-64.

Koirala, M.P., Hayashi, D., 2009. FE modelling along the SAF zone: Implication for the strong/weak SAF, Journal of Geology and Mining Research 1(6), 126-139.

Koirala, M.P., Hayashi, D., 2010. Fault type analysis along the San Andreas Fault Zone: a numerical approach, Journal of Mountain Science, 7, 36-44.

LeFort, P., 1975. Himalayas: the collided range, Present knowledge of the continental arc, American Journal of Science A275, 1- 44.

Li, Q., Liu, M., 2006. Geometrical impact of the San Andreas Fault on Stress and Seismicity in California. Geophysical Research Letters, 33, L08302: 1-4. doi:1029/2005GL025661.

Luo, G., Liu, M., 2009. How does trench coupling lead to mountain building in the Sunandes? A viscoelastoplastic finite element model, Journal of Geophysical Research, 114, B03409, 1-16, doi: 10.1029/2008JB005861

Lynch, J.C., Richards, M.A., 2001. Finite elements models of the stress orientations in well-developed strike-slip fault zones: Implications for the distribution for lower crustal strain. Journal of Geophysical Research 106, 26, 707-26, 729.

Mäkel, G., Walters, J., 1993. Finite-element analyses of thrust tectonics: computer simulation of detachment phase and development of thrust faults. Tectonophysics 226, 167-185.

Malservisi, R., Gans, C., Furlong, K.P., 2003. Numerical modeling of strike-slip creeping faults and implications for the Heyward fault, California. Tectonophysics 361, 121-137.

Manglik, A., Thiagarajan, S., Mikhailova, A. V., Rebetsky, Y., 2008. Journal of Earth System Science, 117 (2), 103-111.

Nelson, K. D., Zhao, W., Brown, L.D., Kuo, J., Che, J., Liu, X., Klemperer, S. L., Makovsky, Y., Meissner, R., Mechie, J., Kind, R., Wenzel, F., Ni, J., Nabelek, J., Leshou, C., Tan, H., Wei, W., Jones, A.G., Booker, J., Unsworth M., Kidd, W.S.F., Hauck, M., Alsdorf, D., Ross, A. Cogan, M., Wu, C., Sandvol, E., Edwards, M., 1996. partially molten middle crust beneath southern Tibet: Synthesis of project INDEPTH results, Science, 274, 1684-1688.

Owens, T. J., Zandit, G., 1997. Implications of crustal property variations for models of Tibetan plateau evolution, Nature, 387, 37-43.

Pandey, M.R., Tandukar, R.P., Avouac, J.P., Lave, J., Massot, P., 1995. Interseismic strain accumulation on the Himalayan crustal ramp (Nepal), Geophysical Research Letters, 22, 751-754.

Pauselli, C., Federico, C., 2003. Elastic modeling

of the Alto Tiberina normal fault (central Italy): geometry and lithological stratification influences on the local stress field, Tectonophysics, 374, 99-113.

Ratschbacher, L., Frisch, W., Liu, G., Chen, C., 1994. Distributed deformation in southern and western Tibet during and after the India-Asia collision. Journal of Geophysical Research 99, 19817-19945.

Schelling, D., Arita, K., 1991. Thrust tectonics, crustal shortening, and the structure of the far-eastern Nepal, Himalaya. Tectonics, 10, 851-862.

Upreti, B.N., 1999. An overview of the stratigraphy and tectonics of the Nepal Himalaya. Journal of Asian Earth Sciences, 17, 577-606.

Yin, A., Harrison, T.M., Ryerson, F.J., Chen, W., Kidd, W.S.F., Copeland, P., 1994. Tertiary structural evolution of the Gangdese thrust system, southeastern Tibet. Journal of Geophysical Research,99, 18175-18201.

Yin, A., Harrison, T.M., Murphy, M.A., Grove, M., Nie, S., Ryerson, F.J., Feng, W.X., Le, C.Z., 1999. Tertiary deformation history of southeastern and southwestern Tibet during the Indo-Asian collision. Geological Society of America Bulletin, 111, 1644-1664

Yin, A., 2006. Cenozoic tectonic evolution of the Himalaya orogen as constrained by along-strike variation of structural geometry, exhumation history, and foreland sedimentation, Earth Science Reviews, 76, 1-131

Zhang, P. Z., Shen, Z., Wang, M., Gan, W., Bürgmann, R., Molnar, P., Wang, Q., Niu,Z., Sun, J., Wu, J., Hanrong, S., Xinzhao, Y., 2004. Continuous deformation of the Tibetan plateau from global positioning system data, Geology, 32, 809-812

Zhao, W., Nelson, K.D., the Project INDEPTH Team, 1993., Deep seismic reflection evidence for continental underthrusting beneath southern Tibet. Nature 366, 557-559

Zhao, S., Müler, R. D., Takahashi, Y., Kaneda, Y. 2004. 3-D finite element modeling of deformation and stress associated with faulting: effect of inhomogeneous crustal structures, Geophysics Journal International, 157, 629-644.